



Trade Science Inc.

Materials Science

An Indian Journal

Full Paper

MSAIJ, 2(6), 2006 [262-267]

Influence Of Fe₂O₃ And MgO As Mineralizers For Tobermorite Synthesis



Corresponding Author

N.Y. Mostafa
 Chemistry Department,
 Faculty of Science, Suez Canal
 University, Ismailia 41522, (EGYPT)
 Tel.: +20-64-382216; Fax: +20-64-322381
 E-mail: nmost69@yahoo.com

Received: 3rd December, 2006

Accepted: 18th December, 2006

Web Publication Date : 27th December, 2006



Co-Authors

E.A. Kishar¹, S.A. Abo-El-Enein²

¹Faculty of Girls, Ain Shams University, Cairo, (EGYPT)

²Chemistry Department, Faculty of Science, Ain Shams University, Cairo, (EGYPT)

ABSTRACT

Tobermorite (Ca₃Si₆O₁₆(OH)₂·4H₂O) crystallites with various morphologies have been successfully synthesized via a hydrothermal process at 175°C for 4 and 24 hours and assisted by Fe₂O₃ and MgO as mineralizers. X-ray diffraction (XRD), scanning electron microscopy (SEM) and Fourier infrared spectroscopy (FTIR) indicated that the mineralizers played a key role in the crystallization and morphology-controlled synthesis of tobermorite crystallites. Mg²⁺ increase crystallinity of tobermorite and change its morphology from platy-shape at 4 hours curing time to lamellar-shape at longer curing time. Fe³⁺ increases imperfection of tobermorite at short curing time, however it increases crystallinity at longer curing time and the morphology of tobermorite change magnificently from reticulated-shape to fiber-shape. FTIR proved that MgO and Fe₂O₃ increase silicate chains polymerization and increase the chain cross-linkage, which is consistent with tobermorite lamellar and fibers morphology that grow parallel to the b-axis (along the silicate chains). MgO and Fe₂O₃ can be used as valuable additives in tobermorite synthesis to tailor the crystal morphology for specific applications like heat insulations with high mechanical properties or used as filters for removal of heavy metal or organic materials from different industrial processes.

© 2006 Trade Science Inc. - INDIA

KEYWORDS

Calcium silicate hydrates;
 Tobermorite;
 Fibers;
 FTIR;
 Substitution.

INTRODUCTION

Tobermorite, $\text{Ca}_5\text{Si}_6\text{O}_{16}(\text{OH})_2 \cdot 4\text{H}_2\text{O}$, is an important crystalline calcium silicate hydrate. The first interest in tobermorite came from its importance in autoclaved building materials^[1-3] and from its resemblance of calcium silicate hydrates (CSH) formed on hydration of Portland cement^[4,5].

Tobermorite commonly synthesised under hydrothermal conditions at temperatures between 100 and 250°C from a silicate and calcium containing materials. Recently, a number of industrial by-products^[6-10] were used for tobermorite synthesis. Microwave hydrothermal synthesis and mechanochemically synthesis have also been investigated as a novel methods for repaid and economical industrial production of tobermorite powder^[11,12].

Tobermorite has three polytypes; 1.4, 1.13 and 0.98 nm, whose names are derived from the approximate d-spacing values of their (002) Bragg reflections (i.e. their basal spacings). The structural unit of all polytypes of tobermorite is an infinite layer of Ca-O polyhedra linked on both sides to infinite Q^2 wollastonite-like silicate chains running parallel to the b-direction^[13-16]. The layers are stacked in the c-direction creating an interlayer region, which accommodates water molecules. The differences between these polytypes (d-spacing) are due to the difference on the number of water molecules per unit formula^[1]. 1.13 nm tobermorite, generally occurs in two varieties; normal and anomalous. The difference between the normal and anomalous types arises from the difference between their thermal behaviors. Both varieties lose interlayer water upon heating to 300°C, but the lattice of normal type shrinks from 1.13 nm to 0.98 nm. The anomalous variety does not shrink. In anomalous tobermorite, the bridging silicate tetrahedra in one chain are bonded to those in the chain across the interlayer region^[17].

To facilitate the description of the silicate structure, researchers^[14,18] use Q^0 - Q^4 notation, which refer to the connectivity. Where Q represents tetrahedron and superscript represents the number of other Q units to which it is bonded. Q^0 refers to isolated SiO_4^{4-} group, Q^1 refers to end group in silicate chain, Q^2 refers to middle group in chain, and so on.

Recently, tobermorite has been investigated for other industrial applications, such as non-asbestos heat insulations^[19], adsorbent for organic or inorganic effluent^[20,21], radio active waste stabilization and cation exchanger^[17,22-24]. Tobermorite used in non-asbestos calcium silicate heat insulations must combine high strength and excellent thermal insulating characteristics. Thus, researchers give attention to synthesis of fibers tobermorite using novel techniques such as Ca-EDTA complex precursor^[25] or microemulsion methods^[26]. These techniques use diluted solutions, high temperatures, long times and special chemicals and instruments, which make them impractical for industrial production.

In our previous study^[2], we found that morphology of tobermorite formed in autoclaved aerated concrete affected markedly with slag additions. Slag contains mainly beside SiO_2 and CaO, Al_2O_3 , MgO, Fe_2O_3 and sulfate. Thus we concluded these components induce a great morphology change in tobermorite. Using Maessbauer spectroscopy, Thomas et al^[27] proved that Fe^{3+} substituted for silica in tobermorite structure. Guangren et al^[28] found in the system CaO-MgO-SiO₂-H₂O at 180°C, tobermorite is the main products. Tobermorite is the only products for samples with MgO/CaO molar ratios less than 0.2. Using EDAX, they give the idealized formula for Mg-tobermorite as $\text{Ca}_{4.36}\text{Mg}_{0.6}\text{Si}_{6.02}(\text{OH})_2 \cdot 4\text{H}_2\text{O}$.

In previous research paper^[29], the effect of Al^{3+} and SO_4^{2-} substitution on tobermorite structure and morphology was investigated. The present research paper investigate the effect of substitution of Mg^{2+} and Fe^{3+} on tobermorite formation morphology under saturated steam pressure.

MATERIALS AND METHODS

CaO was prepared by heating pure grade calcium carbonate at 1100°C for 3 hours, and Min-U-Sil silica is used as silica source (10 μm). All other chemicals are analytical grade. For the preparation of pure tobermorite, calcium oxide (CaO) and silica, with batch compositions of Ca/Si = 0.83 were used as starting materials. This powder mix was added to deionized water, and were quickly loaded into the autoclave. For preparation of Mg^{2+} -substituted and

Full Paper

Fe^{3+} -substituted tobermorite MgO and Fe_2O_3 were used to replaced 2% mole of CaO and SiO_2 respectively.

Teflon-lined steel autoclave 350 cm^3 capacity equipped with magnetic stirrer and heat controller, was used in the preparation^[29]. The hydrothermal syntheses were done using water/solid ratio of 10 at 175°C and curing times 4 and 24 hours. After the hydrothermal treatment, the samples were separated by filtration, washed repeatedly with deionized water, and then dried at 105°C for 24 hours.

XRD analysis were done using a Philips diffractometer (Ni-filtered Cu-K α radiation), at a step size of 0.02°, scan rate of 2° per min, and a scan range from 4° to 50° 2 θ . The powders morphology were investigated using SEM (JOEL, Model: JSM-5600, Japan.) equipped with secondary electron detector and EDX. All samples were coated with gold. FTIR spectroscopic measurements were conducted using a spectrometer (FTIR, JASCO 470). The samples were mixed with KBr with a sample/KBr weight ratio of ~1/100 and compressed to give self-supporting pellets.

RESULTS AND DISCUSSION

XRD analysis

The effect of Fe^{3+} and Mg^{2+} substitutions was investigated at curing time of 4 hours and 24 hours. The products were all tobermorite with almost identical XRD pattern, as shown in figure 1 and figure 2, with no detected quartz or $\text{Ca}(\text{OH})_2$ peaks even for samples autoclaved for only 4 hours (Figure 1). All XRD patterns are drawn with the same scale, thus we can use the relative intensity and the relative broadening in the peaks to compare tobermorite crystallinity. Broadening of 002 peaks corresponds to imperfection in the basal spacing between silicate layers.

Mg^{2+} increases the crystallinity of tobermorite especially at longer autoclaving time (24 hours), as shown in figures 1 and 2.

Figure 1, shows that, Fe^{2+} decrease the crystallinity of tobermorite at short autoclaving time (4 hours). This is due to the increase of imperfection along c-axis (interlayer distances) as indicated by broadening of 002 and 0010 peaks. The same effect

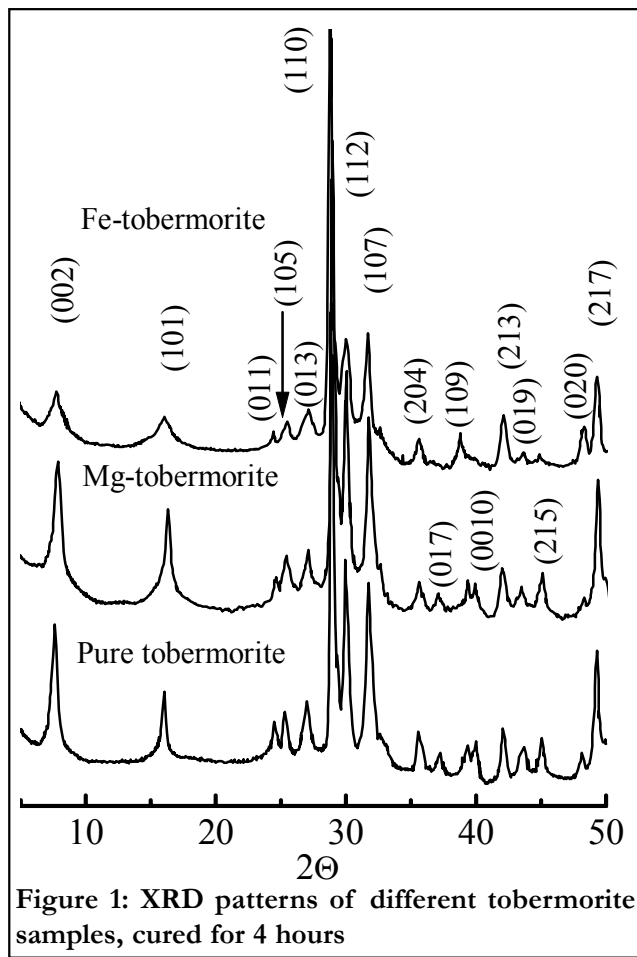


Figure 1: XRD patterns of different tobermorite samples, cured for 4 hours

was found previously^[29] on substitution of Al^{3+} in tobermorite structure. However, the crystallinity of the same sample increases at longer autoclaving time (24 hours), see figure 2. The increase of 002 diffraction intensity, of both Mg-tobermorite and Fe-tobermorite with respect to that of tobermorite without substitution at 24 hours autoclaving, indicates preferred orientation along this crystal planes. This will be explained later in morphology section. High intensity of (00l), (k0l) diffraction and low intensity of (0k0) in the XRD patterns suggested that the obtained tobermorite fibers grow in the b-axis direction.

FTIR spectra

The vibrational spectra of different tobermorite samples are shown in figure 4. Although no carbonates detected by XRD analysis, CO_3^{2-} bands appears in all samples. This due to contamination with CO_2 during samples preparations and drying. Asymmetric stretching of CO_3^{2-} appears as two bands at 1481-

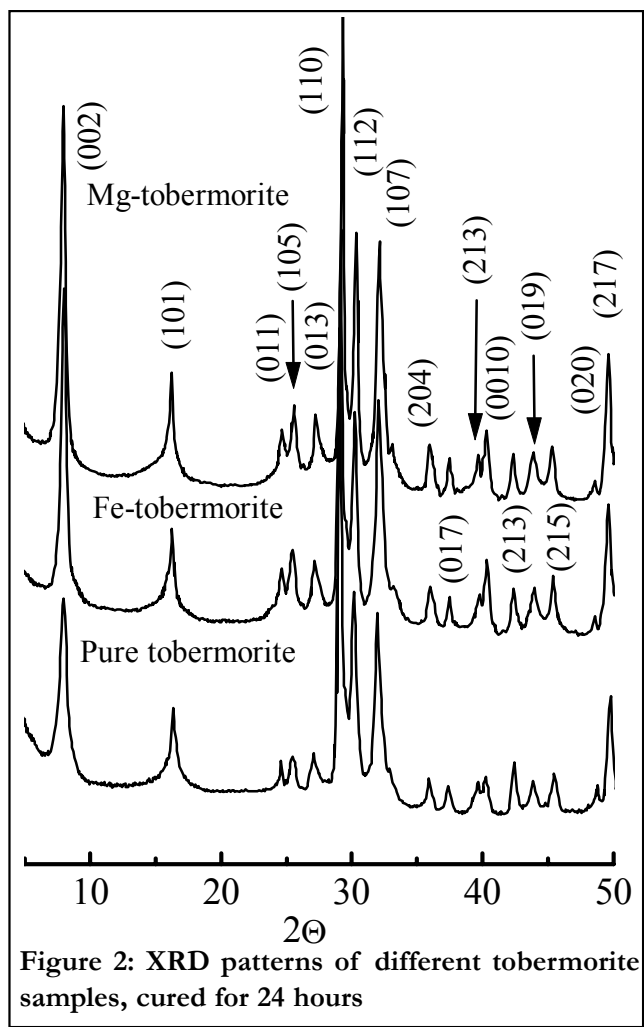


Figure 2: XRD patterns of different tobermorite samples, cured for 24 hours

1414 cm^{-1} .

The bending vibration band of molecular H_2O appears at 1632 cm^{-1} . The stretching vibrations of O-H groups in H_2O or hydroxyls appear as a broad band centered at 3442-3441 cm^{-1} in all tobermorite samples. This broadening is due to the formation of hydrogen bonding with a wide range of strengths^[30-32].

The most intense spectral features of silicates, appear as a complex group of bands in the range of 1100-900 cm^{-1} , attributed to asymmetrical stretching vibrations of SiO_4 tetrahedra^[33,34]. The second most intense silicate bands are broadly characterized as O-Si-O deformation or bending modes, which occur in the 556-400 cm^{-1} region and the band at ~672 cm^{-1} due to Si-O-Si bending vibrations.

Generally, Fe-tobermorite and Mg-tobermorite show better resolved and will defined O-Si-O and Si-O-Si bands than those of pure tobermorite samples. This confirms better crystallinity of both substituted

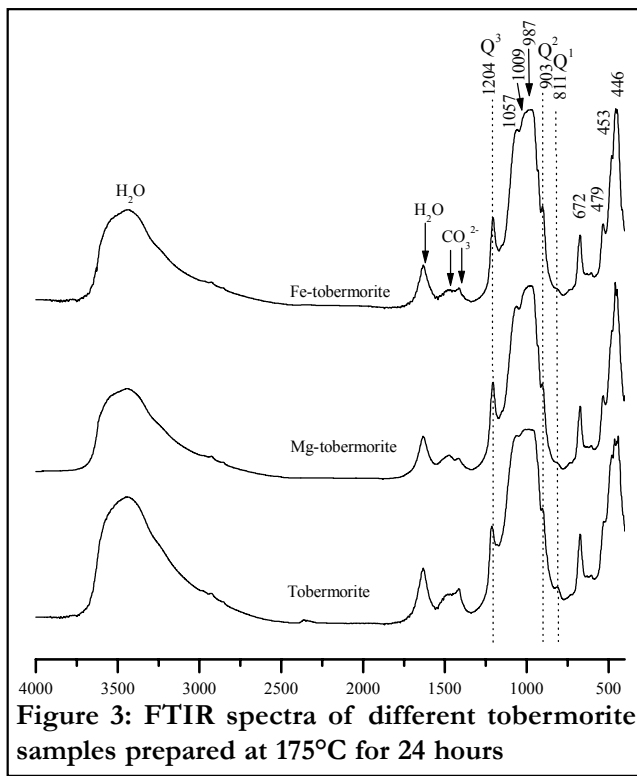


Figure 3: FTIR spectra of different tobermorite samples prepared at 175°C for 24 hours

tobermorite with respect to pure tobermorite sample.

Yu et al^[35] was able to assign different stretching bands of Si-O in calcium silicate hydrates by comparing results from ^{29}Si MAS NMR^[36] and FTIR for the same set of samples. Stretching modes of terminal Si-O bonds; $n(\text{Si-O})$ depends on the connectivity of the silicate tetrahedra^[35]. They assigned band at 811 cm^{-1} to Si-O stretching of Q^1 sites (end chain silicate tetrahedra). This band decreases in Fe-tobermorite and Mg-tobermorite indicating increase of polymerization of silicate chains. These results are consistent with previous investigation^[29], since disordered tobermorite structure contains substantial concentration of Q^1 sites due to the rupture in the silicate chains^[35].

Bands corresponding to Si-O stretching of Q^2 sites appears at 987 cm^{-1} , near 1057 cm^{-1} and 903 cm^{-1} ^[35]. The last band also appears more sharper in Fe-tobermorite and Mg-tobermorite than in pure tobermorite without substitution.

The tobermorite characteristic band near 1200-1204 cm^{-1} , this band is due to Si-O stretching of vibrations in Q^3 sites (silicate tetrahedra link two silicate chain)^[35] This increase with both Mg and Fe substitutions, indicating increase of cross-linkage.

Full Paper

SEM photographs

SEM photographs of tobermorite samples produced by hydrothermal curing for 4 and 24 hours are shown in figures 4 and 5 for Mg-tobermorite and Fe-tobermorite respectively. Pure tobermorite in our pervious study^[29] exhibited small platy crystallites, which are the typical morphology tobermorite^[37]. Tobermorite with Mg substitution exhibit the typical morphology of platy-shape tobermorite at short autoclaving time. This changes to larger lath-like crystallites, at longer autoclaving time as shown in figure 4 (b).

Fe³⁺ substituted tobermorite with reticulated morphology is formed, at short autoclaving time, as shown in figure 5 (a). This reticulated morphology changes to a very crystalline fibers-like tobermorite with increasing processing time up to 24 hours, as

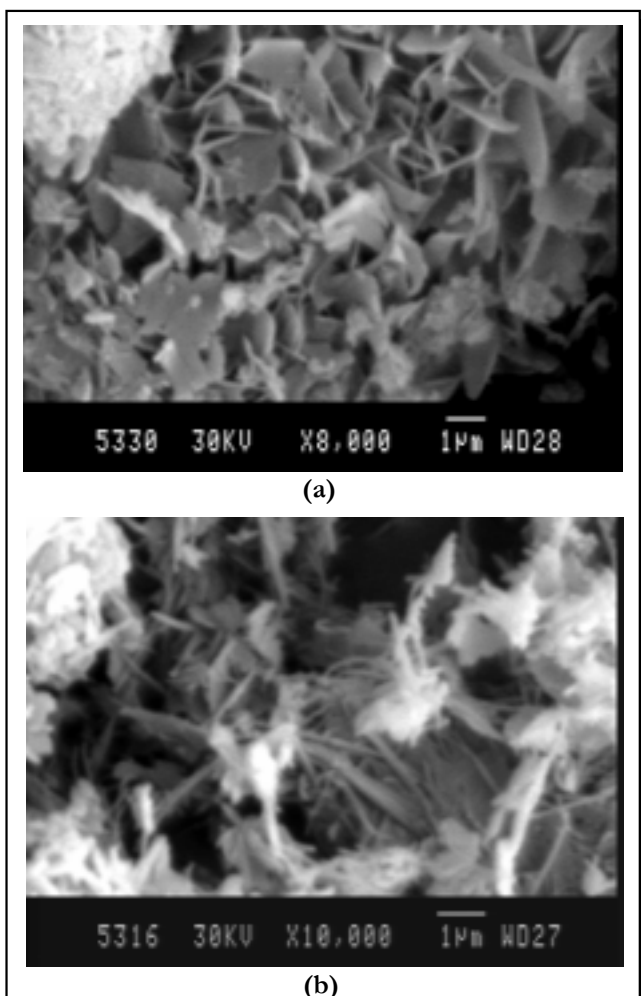


Figure 4: SEM micrographs of Mg-substituted tobermorite; (a) 4 hours (b) 24 hours

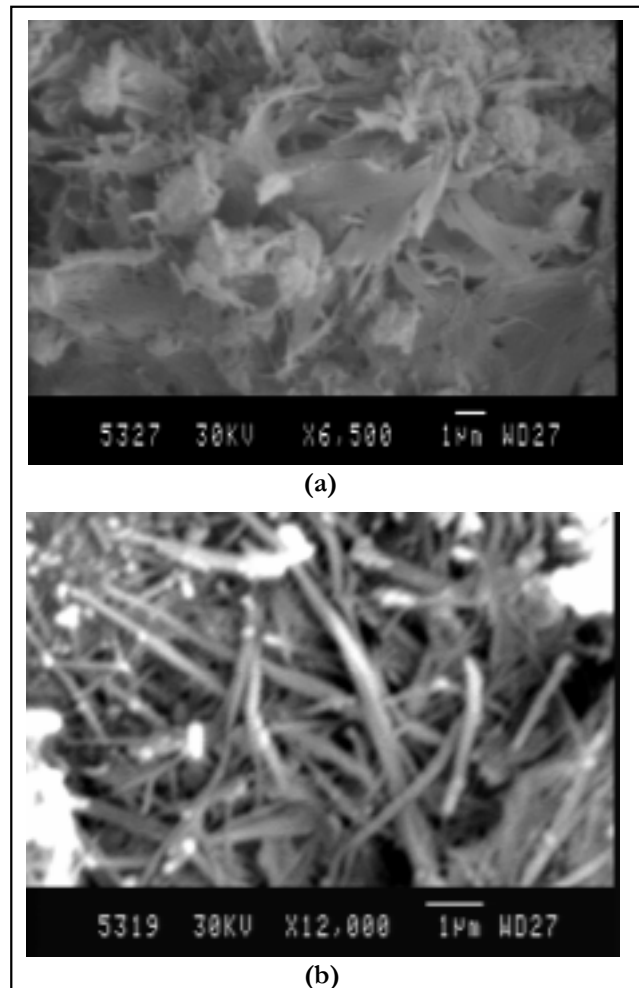


Figure 5: SEM micrographs of Fe-substituted tobermorite; (a) 4 hours (b) 24 hours

shown in figure 5 (b).

CONCLUSION

Tobermorite ($\text{Ca}_5\text{Si}_6\text{O}_{16}(\text{OH})_2 \cdot 4\text{H}_2\text{O}$) crystallites with various morphologies have been successfully synthesized under saturated steam pressure at 175°C for 4 and 24 in stirred suspension. The reaction mixture was modified by substitution of SiO_2 by Fe_2O_3 and CaO by MgO .

Mg^{2+} increase crystallinity of tobermorite and change its morphology from platy-shape at 4 hours curing time to lamellar-shape at longer curing time. Fe^{3+} increases imperfection of tobermorite at short curing time, however it increases crystallinity at longer curing time and the morphology of tobermorite change magnificently from reticulated-shape to fiber-shape. FTIR proved that MgO and Fe_2O_3 in-

crease silicate chains polymerization and increase the chain cross-linkage, which is consistent with tobermorite lamellar and fibers morphology that grow parallel to the b-axis (along the silicate chains). MgO and Fe₂O₃ can be used as valuable additives in tobermorite synthesis to tailor the crystal morphology for specific applications like heat insulations with high mechanical properties or used as filters for removal of heavy metal or organic materials from different industrial processes.

REFERENCES

- [1] H.F.W. Taylor; 'The Chemistry of Cement', Academic Press, London, U.K., (1997).
- [2] N.Y. Mostafa; Cem. Concr. Res., **35**, 1349 (2004).
- [3] E.I. Al-Wakeel, S.A. El-Korashy, S.A. El-Hemaly, N.Y. Mostafa; Cem. Concr. Composites, **21**, 173 (1999).
- [4] H.F.W. Taylor; Adv. Cem. Bas. Mater., **1**, 38 (1993).
- [5] X.D. Cong, R.J. Kirkpatrick; Adv. Cem. Bas. Mater, **3**, 144 (1996).
- [6] C. Tamura, Z. Yao, F. Kusano, M. Matsuda, M. Miyake; Journal of the Ceramic Society of Japan, **150** (2000).
- [7] W. Ma, P.W. Brown; Advances in Cement Research, **9**, 9 (1997).
- [8] N.J. Coleman; Materials Research Bulletin, **40**, 2000 (2005).
- [9] N.Y. Mostafa, S.A.S. El-Hemaly, E.I. Al-Wakeel, S.A. El-Korashy, P.W. Brown; Cem. Concr. Res., **31**, 905 (2001).
- [10] N.J. Coleman, D.S. Brassington; Materials Research Bulletin, **38**, 485 (2003).
- [11] S. Komarneni, J.S. Komarneni, B. Newalkar, S. Stout; Mater. Res. Bull., **37**, 1025 (2002).
- [12] V.V. Boldyrev; Powder Technol., **112**, 247 (2003).
- [13] H.D. Megaw, C.H. Kelsey; Nature, **177**, 390 (1956).
- [14] S.A. Hamid; Z. Kristallogr, **154**, 189 (1981).
- [15] S. Merlino, E. Bonaccorsi, T. Armbruster; Am. Mineral, **84**, 1613 (1999).
- [16] S. Merlino, E. Bonaccorsi, T. Armbruster; Eur. J. Mineral., **13**, 577 (2001).
- [17] S. Komarneni, M. Tsuji; J. Am. Ceram. Soc., **72**, 1668 (1989).
- [18] W. Wieker, A.R. Grimmer, M. Winkler, M. Magi, M. Tarmak, E. Lippmaa; Cem. Concr. Res., **12**, 333 (1982).
- [19] P.G. Walter; United States Patent, 4, 128, 434, December 5, (1978)
- [20] S. Kaneco, K. Itoh, H. Katsumata, T. Suzuki, K.M. Asuyama, K. Funasaka, K. Hatano, K. Ohta; Environ. Sci. Technol., **37**, 1448 (2003).
- [21] Y. Song, U. Berg, P.G. Weidler, D. Donnert, G. Beuchle, R. Nuesch; Proceedings of the 11th Gothenburg Symposium, November, 8.-10th, Orlando, Florida, USA, IWA Publishing, (2004).
- [22] O.P. Shrivastava, R. Shrivastava; Cem. Concr. Res., **31**, 1251 (2001).
- [23] N.J. Coleman, D.S. Brassington, A. Raza, A.P. Mendhamb; Waste Management, **26**, 260 (2006).
- [24] N.J. Coleman; Separation and Purification Technology, **48**, 62 (2006).
- [25] X. Huang, D. Jiang, S. Tan; J. Eur. Ceram. Soc., **23**, 123 (2003).
- [26] K. Lin, J. Chang, J. Lu; Materials Letters, **3**, 342 (2006).
- [27] P. Thomas, S. Komarneni, E. Breval, D.M. Roy L.N. Muly; Materials Research Bulletin, **20**, 1393 (1985).
- [28] Q. Guangren, X. Guangliang, L. Heyu, L. Aimei; Cem. Concr. Res., **27**, 315 .
- [29] N.Y. Mostafa; Effect of Al³⁺ and SO₄²⁻ Substitution on Tobermorite Structure and Morphology, submitted to Materials Chemistry and Physics, November, (2006).
- [30] M. Hanke; Appl. Spectrosc., **40**, 871 (1986).
- [31] J.D. Russell, A.R. Fraser; 11-67, in 'Clay Mineralogy: Spectroscopic and Chemical Determinative Methods', Edited by M.J. Wilson, Chapman Hall, London, U.K., (1994).
- [32] P.F. McMillan; 131-55 in 'Volatiles in Magmas, Reviews in Mineralogy', **30**, Edited by M.R. Carroll, J.R. Holloway, Mineralogical Society of America, D.C. Washington, (1994).
- [33] V.C. Farmer; 'Chemistry of Cement', Ed. H.F.W. Taylor, **II**, Chap. 23, 289 (1964).
- [34] Y. Kudoh, Y. Takeuchi; Min. J., **9**, 349 (1979).
- [35] P. Yu, R.J. Kirkpatrick, B. Poe, P.F. McMillan, X. Cong; J. Am. Ceram. Soc., **82**, 742 (1999).
- [36] X. Cong, J. Kirkpatrick; Adv. Cem. Bas. Mater., **3**, 144 (1996).
- [37] N.S. Bell, S.G. Venigalla, M. Petra, J.H. Adair; J. Am. Ceram. Soc., **79**, 2175 (1996).